

PAPER

Initial results from solenoid-free plasma start-up using Transient CHI on QUEST

To cite this article: K Kuroda *et al* 2018 *Plasma Phys. Control. Fusion* **60** 115001

View the [article online](#) for updates and enhancements.







IOP | ebooksTM

Bringing you innovative digital publishing with leading voices to create your essential collection of books in STEM research.

Start exploring the collection - download the first chapter of every title for free.

Initial results from solenoid-free plasma start-up using Transient CHI on QUEST

K Kuroda¹ , R Raman² , K Hanada¹, M Hasegawa¹, T Onchi¹, M Ono³, B A Nelson², T R Jarboe² , M Nagata⁴, O Mitarai⁵, K Nakamura¹, H Idei¹, J Rogers², S Kawasaki¹, T Nagata¹, A Kuzmin¹, S Kojima¹, C Huang¹, O Watanabe¹, A Higashijima¹, Y Takase⁶, A Fukuyama⁷  and S Murakami⁷

¹ Research Institute for Applied Mechanics, Kyushu University, Kasuga, 812-8580, Japan

² Department of Aeronautics and Astronautics, University of Washington, Seattle, WA, United States of America

³ Princeton Plasma Physics Laboratory, Princeton, NJ, United States of America

⁴ Department of Electrical Engineering and Computer Sciences, University of Hyogo, Japan

⁵ Institute for Advanced Fusion and Physics Education, Japan

⁶ Graduate School of Frontier Science, University of Tokyo, Japan

⁷ Graduate School of Engineering, Kyoto University, Japan

E-mail: kuroda@tri.am.kyushu-u.ac.jp

Received 18 April 2018, revised 12 August 2018

Accepted for publication 24 August 2018

Published 14 September 2018



CrossMark

Abstract

Initial results from the recently implemented transient coaxial helicity injection (CHI) system on QUEST are reported. QUEST uses a new CHI electrode configuration in which the CHI insulator is not part of the vacuum boundary, making this configuration easier to implement in fusion reactors. Experimental results show that transient CHI startup in this alternate electrode configuration is indeed possible. Reliable gas breakdown was achieved, and toroidal currents up to 45 kA were generated.

Keywords: non-inductive current drive, coaxial helicity injection, spherical tokamak, solenoid free fusion plant, electron cyclotron heating

(Some figures may appear in colour only in the online journal)

1. Introduction

Conventional tokamaks rely on the use of a central solenoid to generate the initial plasma current. Non-inductive current drive on tokamaks is an important capability, which increases the prospects of a tokamak for a future fusion reactor. Thus far, in conventional aspect ratio devices, after initial plasma start-up, operation with ~ 700 kA of non-inductive current drive without using the central solenoid has been demonstrated in JT-60U [1]. A compact, low aspect ratio fusion reactor without a central solenoid would have the advantages of lower construction cost and higher plasma beta [2].

In spherical tokamaks, due to space restrictions for a central solenoid, non-inductive plasma start-up without the center solenoid is more crucial. Plasma start-up using microwaves has been confirmed on LATE [3], MAST [4], and QUEST [5, 6]. Non-inductive current drive will also be

studied in NSTX-U [7, 8] and MAST-U [9]. In some of these scenarios the toroidal plasma current evolves through a sequence of non-inductive current ramp phases until it is fully sustained using non-inductive current drive methods.

Transient coaxial helicity injection (CHI) [10] is a promising method for the initial seed current generation in a non-inductive current ramp-up scenario. The CHI current is generated by applying voltage across two coaxial electrodes that are connected by open magnetic flux [11], known as the injector flux. The combination of the injector flux with the external toroidal magnetic field results in a helical field line path encircling the major axis. The injector current supplied by an external power source is driven along the field lines connecting the electrodes. Similar to the situation in a rail gun, the injected current along the magnetic field lines creates a magnetic field with a toroidal component. One may think of the metal armature in a rail gun being replaced by a plasma

Table 1. Primary transient CHI program objectives on QUEST.

CHI Parameters	Required hardware capability
Demonstrate closed flux formation by generating 30–50 kA closed flux current	Using present capabilities
Show that ECH is able to heat a CHI target by comparing the electron temperature of reference CHI plasmas to CHI plasma heated using ECH	400 kW ECH capability
Increase the closed flux current magnitude to ~ 100 kA ($T_e > 20$ eV)	-Increase the toroidal field to ~ 0.4 – 0.5 T -Possibly, lower the electrode plate to be closer to the lower divertor coils or add an additional CHI-dedicated coil
Increase the electron temperature to over 100 eV ($n_e < 9.8 \times 10^{18} \text{ m}^{-3}$)	Replace stainless-steel electrode plate with tungsten electrode plate and include wall conditioning efforts to reduce the presence of low-Z impurities such as from oxidized metal surfaces
Sustain the CHI produced current for longer durations using non-inductive current drive	With the above improvements, and improved knowledge of ECH current drive that is developed in parallel using non-CHI targets

armature consisting of the injector flux. The poloidal component of the current in the plasma load (or the radial component between coaxial electrodes) crossed with the toroidal component of the magnetic field generates the accelerating force. When the injector current exceeds a threshold so that the force, $J_{\text{POL}} \times B_{\text{Tor}}$ overcomes the magnetic field line tension of the injector flux, the injector flux evolves upwards into the vessel carrying with it the injected current.

In transient CHI, soon after the injector flux (the poloidal flux) fills the vessel, the injector current is rapidly reduced to zero. If the injector flux footprints are sufficiently narrow, the injected flux can disconnect at the electrodes, in which case the injected flux inside the vessel can close in on itself and generate a closed field line configuration [12, 13]. The method, referred to as *transient* CHI, is capable of robust and reliable current start-up. On HIT-II about 100 kA of the initial CHI produced toroidal plasma current was ramped up to 180 kA using the central solenoid; this was about 40% higher than the plasma current that was generated by induction alone [10]. On NSTX about 200 kA of the initial CHI followed by inductive ramp up produced toroidal current of 1 MA using 40% less central solenoid inductive flux [14, 15]. If electron cyclotron heating (ECH) is used to heat the CHI plasma, the capability of CHI for current startup is projected to be significantly enhanced. In a scenario of the fully non-inductive current drive, applications of CHI will require ECH heating to increase the electron temperature to the 1 keV level [8].

CHI capability has now been implemented in the mid-size spherical tokamak (ST) device—QUEST [16, 17]. In QUEST, the toroidal plasma current is usually generated by ECH, with minimal use of the central solenoid [18–21]. Without using the central solenoid, a steady state discharge was maintained for more than 1 h 55 min with $I_p \sim 5$ kA of toroidal plasma current [17, 19] by using the 8.2 GHz microwave ECH system [22], and the toroidal plasma current up to about 70 kA has been transiently achieved [21] by using the 28 GHz microwave ECH system [23]. A primary objective on QUEST is to generate about 100 kA of initial

CHI-produced plasma current and to investigate the coupling of this plasma to the 28 GHz microwave ECH system.

QUEST is equipped with important capabilities that will extend CHI studies to new parameter regimes. These are the benefits of CHI operation using a full metallic system that, due to reduced low-Z impurities, should permit the initial plasma to reach higher electron temperature. The capability on QUEST to heat this initial target with ECH should further increase the electron temperature of these plasmas. As described in section 2.1, the CHI electrode configuration on QUEST is simpler and different from the ones on HIT-II and NSTX, and it may be easier to implement this configuration in a fusion reactor [24]. However, CHI start-up in this new electrode configuration needs to be demonstrated. This demonstration would require showing the presence of about 30–50 kA of unambiguous closed flux current after the CHI system is fully turned off, which is signified by the presence of an injector current that is nearly zero. This is an important part of the CHI program on QUEST.

The primary transient CHI objectives on QUEST are shown in table 1. The methodology for this sequence is as follows. First, based on results from HIT-II and NSTX, our understanding of the transient CHI process is that the maximum amount of closed flux current that can be generated in a ST is directly proportional to the amount of poloidal flux that can be injected into the vessel. In addition, through the appropriate use of the injector flux shaping coils, the injector flux must be made sufficiently narrow so that when the injector current is rapidly reduced, the injector flux simply does not pull back into the injector region. On QUEST, the maximum levels of useful injector flux permitted by the present coil configuration are on the order of 28 mWb. Based on results from NSTX [14], the normalized closed flux plasma inductance could be expected to be in the range of 0.35–0.45. For a plasma major radius of 0.64 m, and a flux conversion efficiency of 60%, equation (3) in [14] results in a maximum closed flux plasma current of 100 kA. The flux conversion efficiency is the amount of initial injected open flux that is converted to closed flux. Through careful design

of the poloidal flux coil locations with respect to the CHI electrodes, this conversion efficiency could be made very high, and values above 70% have been observed on NSTX. However, the coil configuration optimization for QUEST CHI is not as good as on NSTX, so that we use a reduced efficiency factor of 60% for QUEST transient CHI. So, this is approximately the highest levels of closed flux current one may expect from QUEST transient CHI experiments. However, for the purpose of demonstrating that closed flux surfaces have in fact been generated in this new electrode configuration, one only needs to show that some unambiguous level of closed flux current is present within the plasma discharge. On QUEST, any persisting current level above 10 kA should be unambiguous, and may be adequate for this initial objective. The 30–50 kA listed in table 1 is a level that is comparable to the levels of current generated by other means on QUEST, such as for example from ECH, so this is used as a target value for a transient CHI demonstration [21]. Since QUEST has a 400 kW of capability of ECH system, showing that ECH is able to heat a CHI target is the next logical step. Finally, getting to 100 kA will require some additional hardware improvements as noted in table 1. For the initial CHI work on QUEST we are using stainless steel electrodes. Metals, in particular iron, have a tendency to oxidize, and at present no specific measures have been taken to control impurities on the electrode plates. However, once the high-current capability of transient CHI on QUEST has been demonstrated, the next logical step is to try and sustain this current non-inductively. For that objective, we plan to implement further improvements such as the use of refractory electrodes and introduce plasma wall conditioning techniques, specifically aimed at improving electrode surfaces to minimize the level of low- Z oxidized impurities, and to reduce electrode sputtering, both of which are needed to reduce radiative losses and to allow the plasma to heat up to high temperatures so that the resulting L/R current decay time could be longer.

This paper expands on the work of the first transient CHI experiments on QUEST, which were reported in the short Rapid Communication paper [25]. In this paper, we describe the CHI system in much more detail, including the conditions needed for initial gas breakdown, the bubble burst current requirements, and the current multiplication factor on QUEST. Then as a result of further improvements to the CHI power supply we were able to generate discharges in which the CHI produced toroidal current magnitude was increased from 29 to 45 kA with evidence for toroidal current persistence after the injector current was reduced to zero.

2. The CHI system on QUEST

QUEST is a mid-size ST device with major radius $R = 0.64$ m and minor radius $a = 0.4$ m. In physical dimensions, it lies between HIT-II ($R = 0.3$ m, $a = 0.2$ m) and NSTX ($R = 0.86$ m, $a = 0.66$ m). On QUEST, as shown in figure 1(a), there are end-plates (divertor plates) on the upper and lower parts of the vessel, and hot walls inside the outer

vessel structure for controlling the temperature of the out-board plasma facing portions of the vessel. During the CHI experiments, the hot wall components were maintained at room temperature. The nominal toroidal field at the machine axis (at $R_0 = 0.64$ m) is 0.25 T in all experiments reported here.

Four poloidal coil pairs located above and below the vessel mid-plane are used to control the plasma equilibrium. These coils are normally operated in a series configuration, with two coils connected to a single power supply. Thus, for example, PF1 and PF7 are connected in series and operated by a single power supply. Likewise, PF2 and PF6 are connected in series, PF3–2 and PF5–2 are connected in series and PF3–1 and PF5–1 are connected in series. The very first CHI experiments on QUEST, described at the beginning of section 3.2 used this configuration. For the more recent experiments that are described towards the end of section 3.2, the PF5–2 and the PF3–2 coils were disconnected from the series configuration and they were driven independently using a dedicated power supply for each coil. This change was implemented to give greater control over the generation of the injector flux.

The microwave injector ECH systems operate at 28 GHz, 8.2 GHz and 2.45 GHz respectively. During the CHI experiments, the 8.2 GHz microwave system was used for pre-ionization to assist with gas breakdown. Figure 1 shows the location of the installed CHI electrodes on QUEST. An external capacitor-based power supply shown in figure 2 and CHI-specific gas injector system were also installed to enable transient CHI operations.

2.1. New CHI electrode configuration

The previous CHI electrode structures are shown for HIT-II in [26, 27] and for NSTX in [14, 28]. Two toroidal ceramic breaks are interposed between the inner vessel (which is the inner cathode electrode) and the outer vessel (which is the outer anode electrode) in these devices. The injector flux connecting the lower inner and outer divertor plates is formed in the injector region by the divertor poloidal field coils. In QUEST, as shown in figure 1, the electrode configuration is simpler in design compared to the ones on HIT-II and NSTX. In QUEST an electrically insulated bias-electrode is installed as a cathode on the lower end-plate and a ground-electrode is attached as an anode to the hot wall which is connected electrically to the vessel.

To achieve the required electrode insulation from the rest of the vessel components, a toroidal-segmented alumina insulator was installed on top of the QUEST lower divertor plate. The insulator consisted of sixteen interlapping arc segments, so that there was no physical gap through the insulator segments. The insulator plate is 42 cm wide (radially) and it was positioned to be aligned with the outer edge of the lower divertor plate. On top of this, a stainless steel current interface plate with a width (radially) of 27 cm was installed. This was also aligned with the outer edge of the lower divertor plate. Then, at three toroidal locations, the current interface plate was connected to the current feed rod

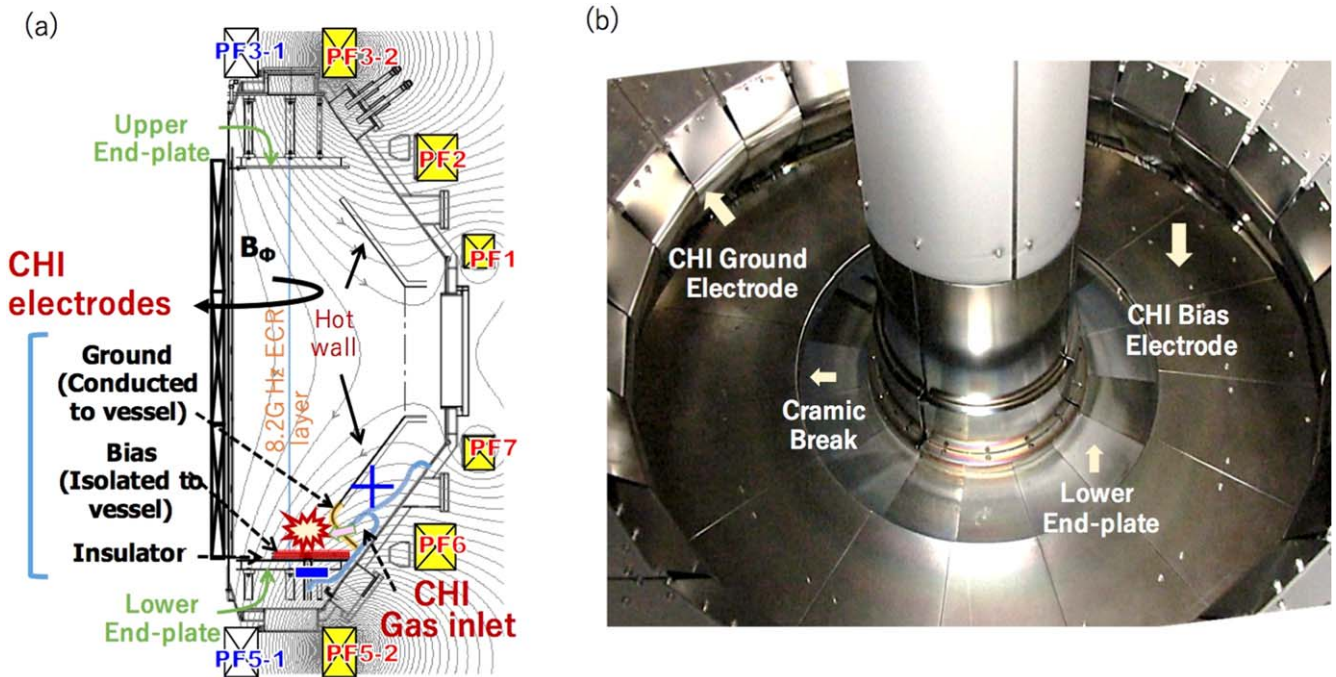


Figure 1. The new CHI system in QUEST. (a) Side view of the QUEST drawing showing the upper and lower end-plates, hot walls, and CHI (bias and ground) electrodes. Gray contours indicate typical magnetic flux surfaces formed by poloidal field coils (PF1-7) and the cyan line shows the location of the ECR layer of 8.2 GHz microwave used for pre-ionization. (b) Photo of CHI electrodes in QUEST.

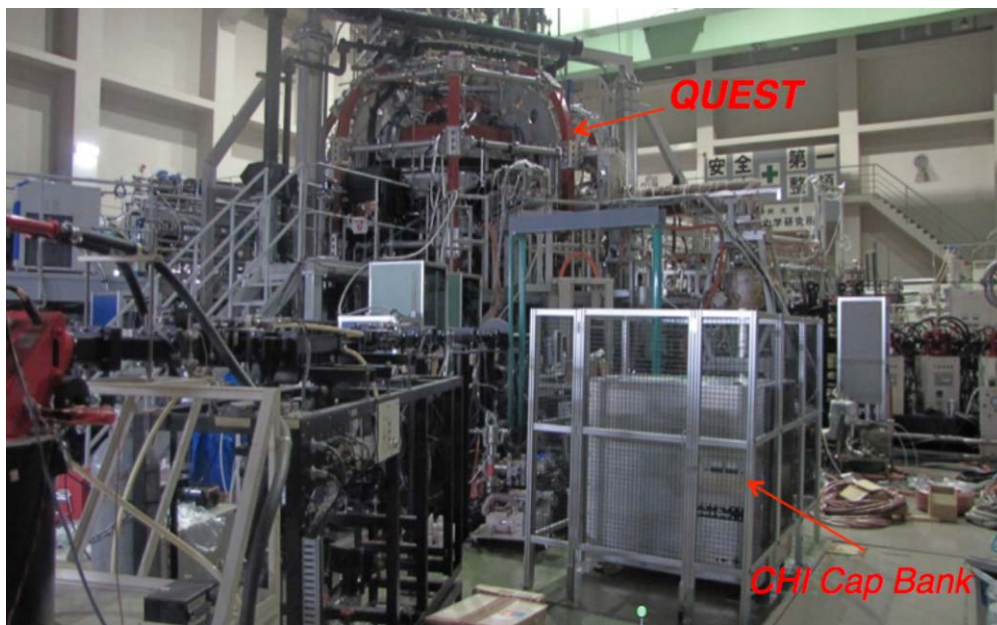


Figure 2. Photo showing the QUEST device and the 2 kV, 30 mF CHI capacitor bank power supply. The power supply is located about 10 m away from the QUEST vessel. Six coax cables (RG218 equivalent) are used to connect the power supply to the CHI electrodes on QUEST.

that extended all the way down below the lower vessel components on QUEST. An alumina insulator tube surrounded the current feed rod, and the vacuum interface for the three current feed rods was made at the lower part of the entrance into the QUEST vessel. A custom vacuum feedthrough design was used to provide capability for the insulating feedthrough to move without adding stress to the insulating ceramic tube. The primary component of the insulating feedthrough is PEEK (Polyether ether ketone).

Three current feed locations were chosen to reduce the total maximum current through each rod to accommodate the $J \times B$ forces on the rods during operation with an external toroidal field. Finally, an electrode plate also 42 cm in width (radially) was installed on top of the current interface plate and bolted on to the current interface plate. The cathode electrode plate has the same inner and outer diameter as the alumina insulator plate. The alumina plates were not radially extended past the edge of the electrode plate to avoid direct

plasma contact during normal (non-CHI) QUEST plasma operations.

In general, it is preferable to install the CHI electrode closer to the center stack region so that CHI could benefit from the higher levels of toroidal field that are present in this region. But because CHI was not part of the original QUEST design, and due to the need for minimizing changes to the QUEST physical hardware and the added benefits of locating it closer to the lower external poloidal field coils, the electrode plate was positioned to be aligned with the outer edge of the lower divertor plate.

The PF5-2 coil is used as the primary coil to generate the injector flux. PF coils adjacent to PF5-2 are used to shape the injector flux. The injector flux connects the lower end-plate electrode (the cathode) to the ground electrode attached to the hot-wall components. The NSTX as well as the QUEST types of CHI electrode designs have been considered for application of transient CHI to an ST-FNSF [29] based fusion power plant [24]. The performance of CHI current drive on the former (NSTX type) electrodes is easy to predict from the experimental results from HIT-II and NSTX, but that electrode configuration requires a more complicated design for electrical insulation. A main goal of the CHI experiments on QUEST is to investigate the performance of the current drive using the alternate simpler electrodes to facilitate the application of transient CHI in a fusion reactor.

2.2. Power supply and control system

The transient CHI system on QUEST is powered by a capacitor bank containing six 5 mF, 2 kV capacitors. The maximum bank energy is 60 kJ. The capacitor bank is configured for operation with two Type A ignitrons. Two or three capacitors can be connected to each ignitron. The ignitrons can be triggered independently. This flexibility is needed to provide some voltage programming capability as the CHI discharge evolves in time and is based on experience gained from CHI operations on NSTX that uses a similar capacitor bank configuration. Experience on NSTX showed that if too much capacitor bank energy is discharged when voltage is first applied to the electrodes the plasma evolution is so fast that it just ejects a portion of the plasma all the way to the other end of the vessel and plasma does not have sufficient time to adjust to the equilibrium conditions being provided by the pre-programmed external field coils. Thus, the method developed on NSTX is to first discharge a smaller portion of the capacitor bank energy and allow the plasma to grow part way up the vessel and then discharge an additional capacitor bank module to further grow the plasma.

The capacitor voltage at each of the two ignitrons is monitored, and this information is fed back to a Labview based control system used to operate the capacitor bank. The current output from the capacitor bank is connected to the CHI electrodes at three different toroidal locations using six coax cables. Fast voltage monitors are used to actively monitor the electrode voltage at these three locations during the plasma pulse. The ground side of the capacitor power supply is directly connected to the vessel, which is also the

primary ground during CHI experiments. At each of the current feed locations, a high power 100 Ω resistor is connected directly across the high voltage and ground leads. This is a safety system that allows the ignitrons to conduct even if a plasma load is not established inside the vessel during CHI operations. This system proved very helpful during the initial plasma commissioning experiments on QUEST. To suppress voltage spikes, resistor-capacitor snubbers are also employed at each of the three current feed locations. Each snubber consists of a low inductance 600 mOhm resistor stack in series with a 32 μ F capacitor. The current through each of the ignitrons as well as the total current through both ignitrons (the injector current) is measured.

Figure 3 shows the circuit diagram of the capacitor bank, operated by the Labview based control system. The CHI power supply operation is initiated by first disconnecting the high voltage side of the capacitor bank from ground. This is followed by programming the charging power supply to the desired voltage, then connecting it to the capacitor bank by energizing a relay. After the capacitor bank is fully charged, the charging relay disconnects the power supply from the capacitor bank. At the appropriate time, the main QUEST plasma control system sends a trigger to discharge the capacitor bank. The CHI Labview controller provides a pre-programmed delay between ignitrons 1 and 2 so that the second ignitron can be triggered after some delay, as in NSTX. After the end of the QUEST shot cycle, the capacitor bank is returned to the normal safe state.

2.3. Gas injector and control system

Figure 4 shows the CHI gas injector system. Hydrogen gas enters the injector flux region at two toroidal locations via fast pneumatic valves connected to small plenums. The pneumatic valves are used because solenoid-operated valves cannot be used in the high magnetic field region near the coils. To operate these valves, helium at 0.7 MPa is supplied by solenoid-operated valves 1.5 m away in the lower field region. As shown in figure 1, the gas inlet inside the machine is at the anode. The injected gas is directed towards the high-voltage cathode plate. The timing of the gas injectors is adjusted to provide maximum gas pressure in the inter-electrode region at the time the capacitor bank discharge is initiated.

The gas valves are also operated by the Labview based control system. First, the small gas plenum located between the two pneumatic valves is filled with hydrogen by first ensuring that the fast valve to the QUEST vessel is closed and then opening the slow pneumatic valve for a brief period. The pneumatic valves are activated by pressurizing a gas line using a solenoid valve located in a low magnetic field area. At the required time, the QUEST plasma control system sends a trigger signal to a fast 120 V trigger generator, which rapidly activates the solenoid valve used to trigger the fast valve. At the end of the cycle, the pressurized gas lines between the solenoid valve and the pneumatic valves are vented and the pneumatic valves returned to their normal state.

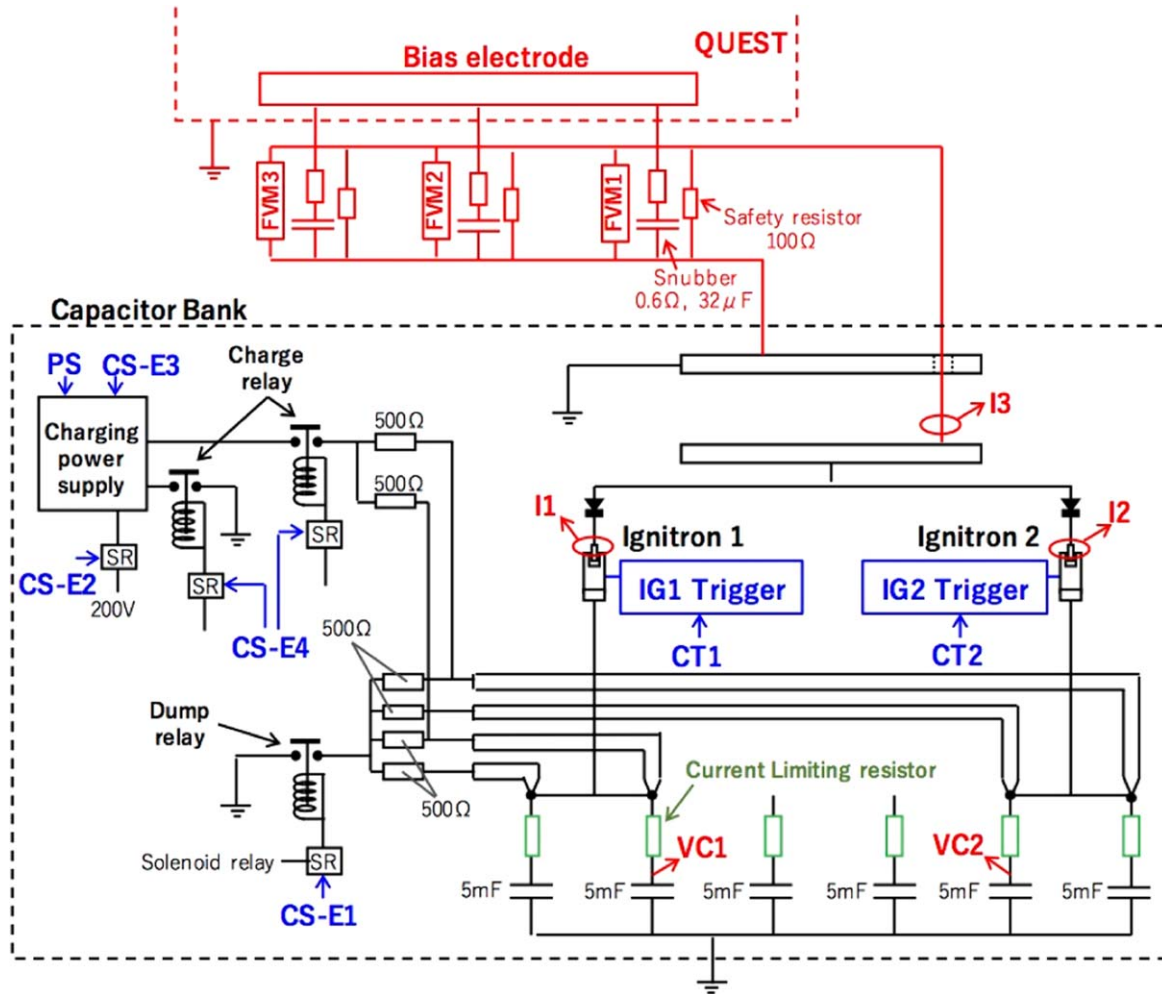


Figure 3. Circuit diagram of the capacitor bank connected to the bias electrode in QUEST. CS-E1, 2, 3 and 4, PS and CT1 and CT2 are control signals from the Labview control system. Voltage of capacitors (VC1 and VC2), currents through ignitron 1 and 2 (I1 and I2) and total current (I3) and electrode voltages at three different toroidal locations (FVM1-3) are monitored.

2.4. CHI discharge operation

The CHI system on QUEST is operated as follows.

- (1) Toroidal field at $B_{T0} = 0.25$ T is applied and then the injector flux configuration is formed by driving currents in the poloidal field coils. A typical injector flux pattern is shown in figure 1.
- (2) H_2 gas is injected into the injector region by gas injectors 1 and 2.
- (3) At the time when the gas pressure in the electrode region reaches a high value (about 18 ms after the trigger timing of the fast valve), voltage in the range of -1.0 to -1.8 kV is applied to the bias-electrode by the capacitor bank power supply. If conditions for gas breakdown are satisfied, the injected gas is ionized and the injector current starts flowing along the injector flux that connects the ground anode to the cathode electrode plate. Triggering the gas valves and observing with a fast camera to see when the gas first begins to breakdown in the injector region is used to adjust the timing.

3. Experimental results and discussion

3.1. Gas breakdown

Reliable gas breakdown was achieved in the injector flux configuration shown in figure 1, with 26 mWb of poloidal injector flux connecting the electrodes. This corresponds to operation with -1.5 kA of coil current in the PF5-2 coil that has 41 turns. If the current in this coil was increased to -2 kA, breakdown was still possible, but it was not very reliable. With -5 kA in the PF5-2 coil breakdown was not possible. All these conditions used about -1.8 kV charging voltage. It was also found that about 20–30 kW of 8.2 GHz ECH was necessary to achieve breakdown. The reason for this dramatic change in breakdown behavior is attributed to the need for satisfying the Paschen condition for gas breakdown [30], and is shown in figures 5 and 6.

Although Paschen's condition was derived for electrical breakdown between flat plates, interestingly, a careful examination of the breakdown requirements for NSTX CHI discharges by Hammond [31], shows that it can also be applied to the CHI configuration, possibly because the

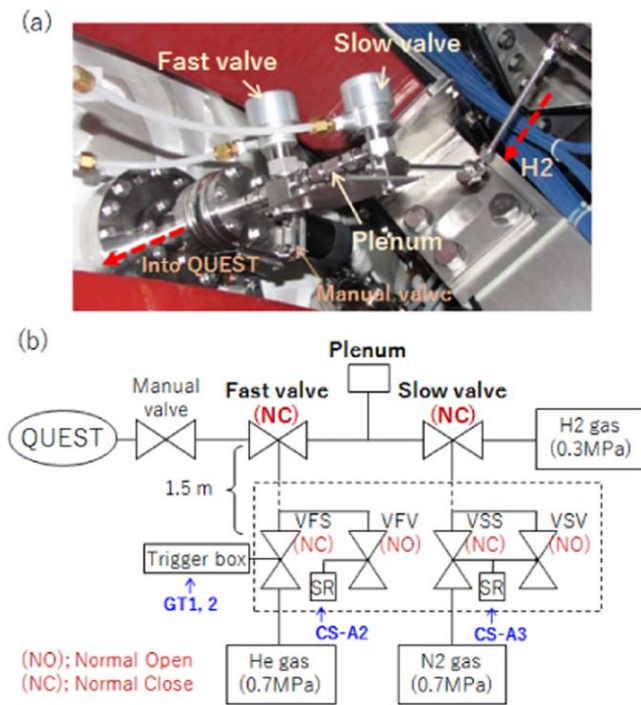


Figure 4. (a) Photo of CHI gas injector. (b) Diagram of gas injector piping lines. CS-A2 and 3 and GT1 and GT2 are the signals from the Labview controller for operation of solenoid valves, VFS, VFV, VSS and VSV.

electron's accelerated speed parallel to the magnetic field due to E_{\parallel} is much higher than the drift speed perpendicular to the field due to E_{\perp} . For QUEST case, the accelerated speed due to E_{\parallel} is $\sim 2 \times 10^7 \text{ m s}^{-1}$ while the drift speed due to E_{\perp} is $\sim 4 \times 10^4 \text{ m s}^{-1}$. On QUEST, a very clear trend has been seen for improved breakdown as the ratio of toroidal flux to injector flux is increased.

Figure 5 is a plot of the field line connection length between the electrodes calculated at the location where the 8.2 GHz ECH resonance layer intersects the high-voltage electrode plate (shown in figure 1). It shows that the field line connection length is 1.3 m for maximum current of -5 kA in the PF5-2 coil but increases to 4 m if the coil current is reduced to -1.5 kA , 30% of its maximum rating. Figure 6 is a plot of the required gas pressure for gas breakdown at -1.8 kV for these two connection lengths. It shows that the required gas pressure in the injector region is nearly 3 times higher for the case of shorter connection length (the high injector flux case). Experimental conditions on QUEST do not allow us to measure the inter-electrode gas pressure, but this calculated pressure requirement, in conjunction with the observed vessel pressure, which is in the $5\text{--}10 \times 10^{-2} \text{ Pa}$ range strongly suggests insufficient gas pressure as the reason for not being able to achieve breakdown at the high injector flux values.

Conditions for breakdown at higher values of the injector flux can be enhanced by improving the response time of the gas injection system so that the gas plenum empties faster: increasing the conductance of the gas pipe line could further increase the gas pressure transiently in the electrode region

while keeping the total amount of injected gas low. Increasing the toroidal field would also increase the field line connection length. In these experiments, the toroidal field was 0.25 T. However, in a pulsed mode, with additional modifications to the power system hardware, QUEST may be able to support operations at 0.5 T.

Although a higher value of the toroidal field (for a given injector flux) increases the field line length and reduces the gas pressure necessary for gas breakdown, it also increases the required voltage to attain a given injector current.

3.2. Toroidal current generation

In this section we describe the results of toroidal current generation in the QUEST CHI electrode configuration. Figure 7 shows the waveforms of a discharge after voltage application by the capacitor bank power supply. The primary observation is that the voltage monitor signals at the three locations on the electrodes are largely the same. The orange trace does show slightly increased amplitude that could be due to some asymmetry in the arcing along the electrode plates. While transient localized arcs are seen in some discharges, the location of this voltage monitor behind the center stack (from the fast camera viewpoint) does not at this time permit us to say if this is due to asymmetry in arcing or due to increased electromagnetic noise pick-up in this channel. Future experiments will try to better understand these small differences in the voltage measurement. Given that the increased amplitude in the orange signal is small, the voltage seems to be applied axisymmetrically to the electrodes, and there are no major asymmetries in the CHI discharge on the electrode plates, even though the gas is injected at only two locations. From an initial value of -1.8 kV near $t = 0$, the voltage drops rapidly to a lower value of about -600 V at $\sim 0.1 \text{ ms}$. The voltage drop signifies gas breakdown. This is the first indicator of the bias-electrode being electrically connected to the vessel ground through a conductive plasma load inside the machine. In conjunction with this voltage drop, the injector current and toroidal current begin to increase. The injector current from ignitron 1 flows first and then, after the delay of 0.1 ms, the current from ignitron 2 also flows. By changing the delay time, the injector current waveform is adjusted. The total plasma current is calculated in two ways. First, by numerically integrating the raw unintegrated signal from a Rogowski coil measurement inside the QUEST vessel. Second, by correcting for integrator droop of the passively integrated Rogowski coil signal. Both these measurements agree with each other. The toroidal current also increases with the injector current and continues to increase up to a peak value of 22 kA as the injector current decays in time. In this early discharge on QUEST, the toroidal current persists for just as long as the injector current is present. Although some toroidal plasma current may flow on closed flux surfaces, we cannot rule out the possibility that all the toroidal current in this case flows on open field lines.

During these discharges an AXUV photodiode array was used to track the motion of the evolving plasma discharge, shown in figure 8. The waveforms show the radiation from

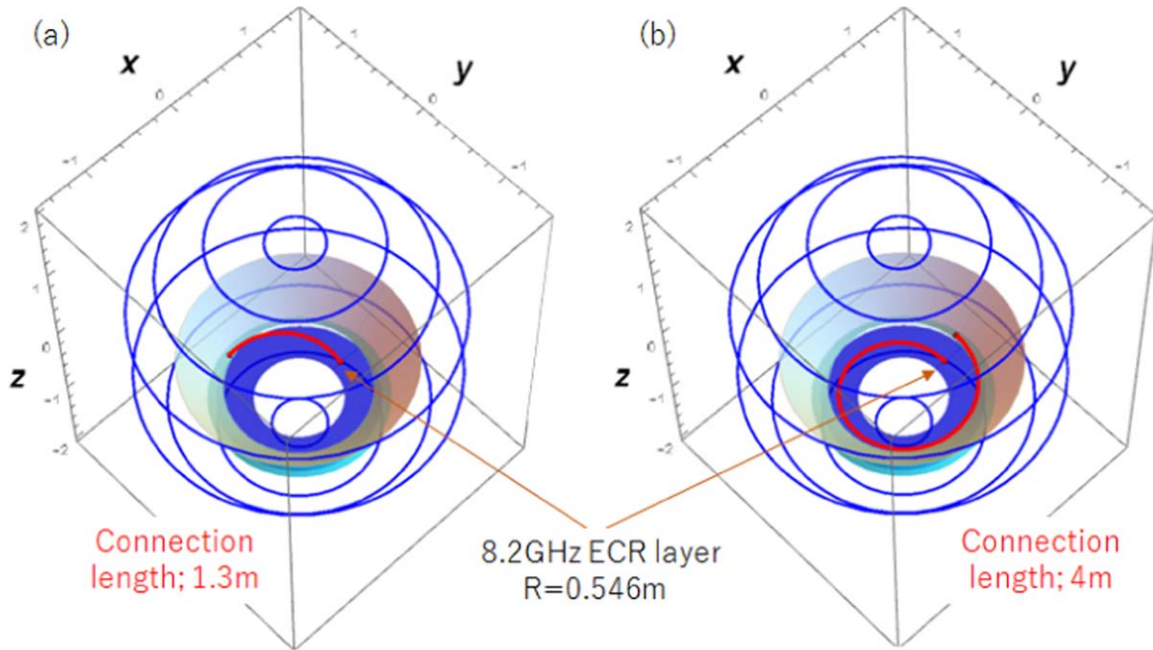


Figure 5. Field line connection length between CHI electrodes at the location where 8.2 GHz ECH resonance layer intersects the high-voltage electrode plate with (a) -5 kA in PF5-2 coil (41 turns), 50 A in PF6 coil (36 turns) and 1 kA in PF7 coil (12 turns) and (b) -1.5 kA in PF5-2, 15 A in PF6 coil and 0.3 kA in PF7 coil. (The toroidal field is 0.25 T.)

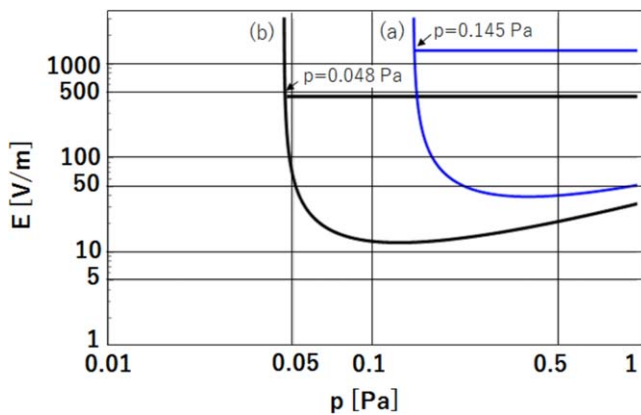


Figure 6. Required gas pressure for gas breakdown at -1.8 kV for two field line connection lengths, (a) 1.3 m and (b) 4 m. Curved lines are the calculated Paschen conditions and straight lines are electric field on each field line.

the visible to the soft x-ray region. The AXUV diode sight lines are shown on the left side of figure 8. The experimental traces are shown on the right side of the figure. The differences in the rising phase of waveforms of the different channels reflect plasma growth crossing the sight lines. A mid-plane camera was also used during these first experiments. The primary observation is that the AXUV diode signals are consistent with the plasma growing up from the injector at least to the mid-plane. The camera measurements were consistent with this but did not have sufficient time resolution to confirm detachment of the plasma from the injector.

The data in figure 7 shows that the CHI produced toroidal current does not track the injector current. The CHI produced toroidal current peaks well after the injector current peaks. The injector current has reduced to a substantially lower level

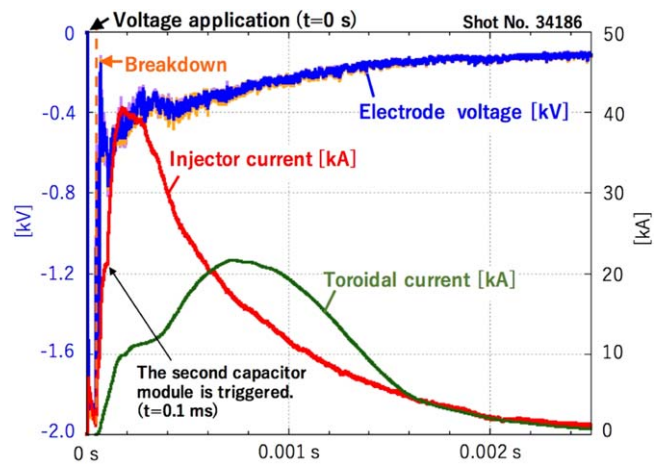


Figure 7. Waveforms of the three voltage monitors across the electrodes, injector current monitored at the outlet of power supply and toroidal current after voltage application by capacitor bank power supply. The trigger time of the second capacitor module can be seen by the inflection in the injector current waveform, and the corresponding changes to toroidal current waveform on a much slower time scale. The plasma current measurement has an error bar of less than 0.5 kA.

at the time of the peak in the toroidal current indicating that, for this low temperature plasma, some closed flux surfaces may be forming but are masked by the long decay time of the CHI injector current. This suggests the need for ramping down the CHI injector current more rapidly. To permit this, the CHI capacitor bank was modified by replacing all twelve current limiting power resistors between capacitors and ignitrons, as shown in figure 3, from 150 mOhms each to 40 mOhms each to reduce the RC discharge time. In addition, the size of the gas injection plenums was reduced and the

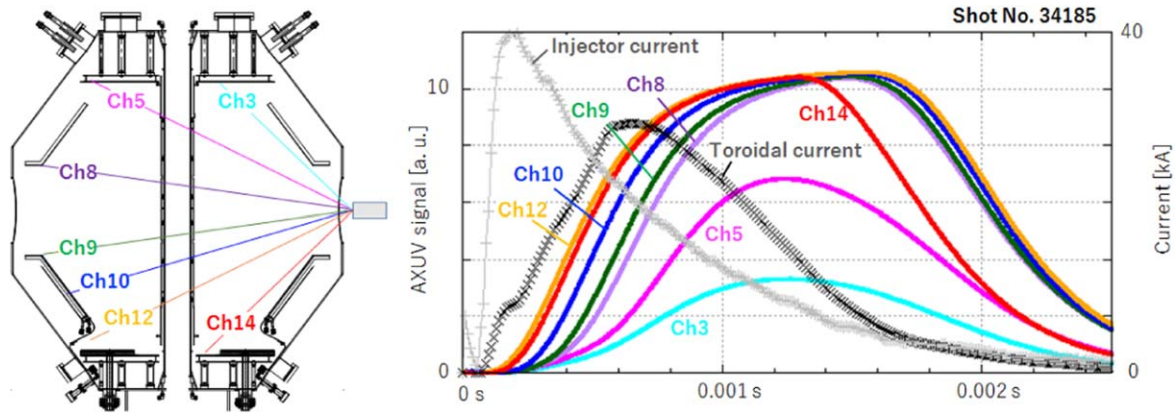


Figure 8. AXUV sight line schematic drawing and the signal from each channel. Black and gray plots show the toroidal current and injector current, respectively.

operating pressure of the gas system increased so that less gas would be injected, but much more rapidly. The power supply configuration for the QUEST PF coils was also changed to provide better control of the CHI plasma discharge. The main injector flux coil (PF5-2) was independently operated, without it being connected to the PF3-2 coil. The currents in the PF1 and PF7 coils, which are responsible for generating the vertical equilibrium field, were increased to better position the plasma inside the vessel. Finally, the camera system was substantially improved by adding a fast color camera, better positioned by using a reentrant lens system that provided more complete coverage of the vessel interior. It is useful to note that due to the reduced series resistance the charging voltage on the capacitor bank must be appropriately reduced to attain the required injector current.

With these operational changes, the CHI discharges improved substantially. The amount of injected gas was reduced to 15 Torr l by a factor of about two compared to the gas injection amounts of 31 Torr l used during the discharge shown in figure 7. Initiation of CHI discharges at sufficiently low levels of injected gas is quite important, and necessary, as described in a recent NSTX CHI paper [31]. Improved toroidal currents up to 45 kA were generated that showed toroidal current persistence after the injector current was reduced to zero, as shown in figure 9. The plasma was generated using 23 mWb of poloidal injector flux, which was formed mainly by driving 2.1 kA of current in the PF5-2 coil. Figure 9 shows that the injector current now drops much faster, and some CHI generated toroidal current remains after the injector current has been reduced to zero. While small, the existence of persistent current is a definite improvement, which was not observed in the early discharges, as shown in figure 7. The error in the toroidal current measurement is less than 0.5 kA, as the toroidal current is zero when there is no gas breakdown. Since the central solenoid is not used to drive a loop voltage and none of the PF coil currents are changed in time during these experiments, there is no source, other than CHI, for toroidal current generation in the plasma or in CHI electrode plate. Figure 9 also shows images from the fast camera observations at different times during the discharge pulse. These show the existence of a plasma throughout the toroidal

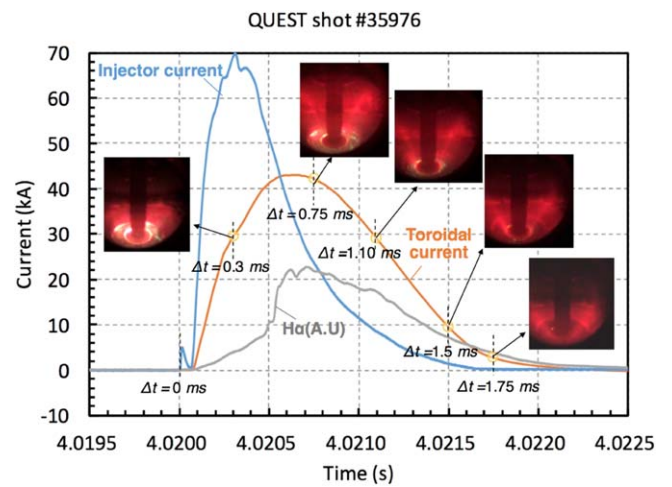


Figure 9. Transient CHI discharge on QUEST that uses a faster injector current ramp-down time. Shown are the CHI produced toroidal current, injector current, H α signal and fish eye fast camera images at different times during the discharge.

current pulse measurements. Data from a mid-plane Halpha chord also show the presence of plasma throughout the pulse, consistent with the camera images. There is a possibility that the small amount of persisting current could be induced in the electrode plate or in the surrounding structures, as the CHI-produced toroidal current decays. However, if this were the primary source of the long small current decay, then one would think that it should be related to the magnitude of the initial CHI-produced toroidal current. This is not the case. The highest CHI produced toroidal currents do not show the longest current decay times. In addition, spectroscopic signals and the visible camera images show the presence of plasma when the current is present. Nevertheless, given the small amount of persisting current that is present, at this time, one cannot completely rule out the possibility that some of the current maybe induced on the vessel and CHI structure. While this is an encouraging initial result, additional improvements to the plasma equilibrium control and the injector flux shaping are needed to improve the current persistence results before one can conclude that this is due to the presence of some

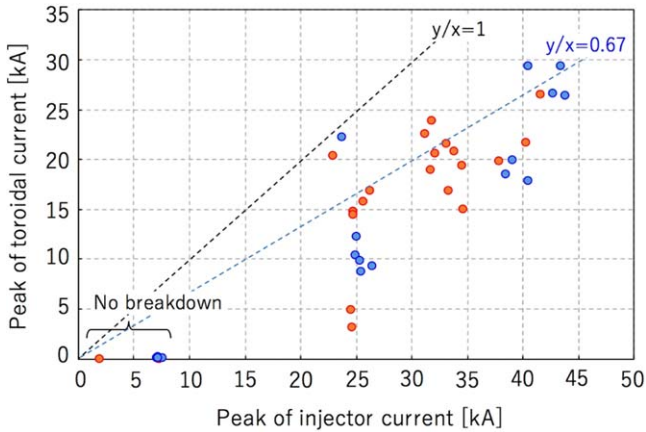


Figure 10. Peak of toroidal current versus peak of injector current for the shots with the same PF 5-2 coil current of -1.5 kA. Orange circles indicate the shots with the typical condition of the other PF coil currents, 15 A in PF2 and PF6 coils (36 turns for each) and 0.3 kA in PF1 and PF7 coils (12 turns for each) and blue circles indicate shots in which there are further changes to these coil currents. A small amount of current flows in the snubber circuit resulting in some injector current even for the no-breakdown cases.

closed flux plasma in the discharge. These results show that the new CHI electrode configuration on QUEST is indeed performing similar to the electrode configurations used on HIT-II and NSTX, although many more improvements remain to be made to attain the level of transient CHI discharge performance attained on HIT-II and NSTX.

3.3. Bubble burst condition and current multiplication ratio

In these CHI discharges the injector current continued to increase with the capacitor bank energy, which is an expected result. Figure 10 shows the peak injector current versus the peak of toroidal current for many shots with the same PF 5-2 coil current of -1.5 kA, but with not the same level of current in the other PF coils. Two to four capacitors were used in these discharges. The figure shows the toroidal current to increase with the injector current. This is an important result as it means that the additional injected power must be driving the main CHI plasma load, and that most of it is not lost in spurious arcs, such as the absorber arcs reported in NSTX CHI plasmas [32]. This is an encouraging result for this alternate electrode configuration used on QUEST. At the same injector current value, there is a large scatter in the measured toroidal current. This is because the equilibrium PF coil currents conditions were not all the same during this initial study. Configurations that have a wider injector flux footprint would require less injector current to grow the plasma, and these aspects have not been studied at this time. In addition, there is also some undesirable arcing in some discharges. These need to be better characterized in future studies.

The data shows that about 25 kA of injector current is needed before the toroidal current begins to increase. This threshold is approximately consistent with the bubble burst current magnitude [11, 13, 33].

Because the injector flux pattern ranges from the outer edge of the electrode to the inner edge, and because the inter-electrode

gap distance also changes as a function of radius, one cannot explicitly calculate a single value for the bubble burst current. Ultimately, one needs to know the current density on these field lines to correctly calculate the bubble burst current. Through consideration of other factors such as the exact geometry of the QUEST electrode, one may in future, be able to improve the bubble burst current calculation. Nevertheless, the bubble burst current parameter provided in [11] is a useful parameter that provides an estimate for the magnitude of the required injector current in CHI discharges. The bubble burst current calculated as $I_{inj}^{BB} = 2\psi_{inj}^2 / (\mu_0^2 d^2 I_{TF})$, with a representative electrode gap of 0.2 m, and injector flux of 26 mWb results in a bubble burst current magnitude of about 26 kA. Here I_{TF} is the current in the toroidal field coil, 800 kA, d is the electrode gap and ψ is the injector flux.

The bubble burst current is the threshold injector current needed to overcome the magnetic field line tension as reported in previous studies of CHI [11]. At this threshold value, the $J_{POL} \times B_{TOR}$ force is able to overcome the field line tension of the injected flux, allowing the currents flowing along these field lines and the injector flux to expand and fill the vessel.

Another observation is that the current multiplication ratio of the peak toroidal current to the injector current peak is lower than 1 for these discharges, whereas it is 6 to 7 on HIT-II and it is up to 70 on NSTX. This is due to a combination of yet un-optimized discharges on QUEST that does not permit a direct comparison with results from HIT-II and NSTX and because of the much lower value of the toroidal flux within a QUEST CHI discharge. Since the current multiplication factor is proportional to the ratio of toroidal flux to the injector flux in the CHI plasma [11], and not to the absolute value of the toroidal field, it is necessary for the discharge to fully fill the vessel before a good comparison could be made to the results from the HIT-II experiment. HIT-II nominally operated with 12 mWb of injector flux and at 0.5 T to achieve a current multiplication of 6. In comparison QUEST has twice the value of the injector flux and half the toroidal field of HIT-II and these discharges do not yet fill the vessel completely, as did the CHI plasmas on HIT-II and NSTX.

Simple estimates that consider a circular plasma with minor radius in the range of 10–20 cm show that such a plasma would have enclosed toroidal flux in the range of 8–30 mWb. This is similar to the magnitude of the injector flux. So, we would expect the current multiplication factor to be in the range of one for these first experiments. In future experiments as larger bore plasmas are generated, and the plasma expands to more fully fill the vessel, and with less injector flux, the current multiplication factor should exceed 1, and reach about 3, even at only 0.25 T toroidal field.

4. Summary

Initial experimental results from transient CHI plasma generation using a new electrode configuration on QUEST are very encouraging for future CHI plasma start-up studies on

QUEST. Reliable plasma breakdown and poloidal flux evolution into the vessel have been demonstrated, which shows that CHI plasma evolution in the new electrode configuration is indeed possible. This is an important, and necessary, first step to enable useful CHI plasma operations on QUEST. The maximum achieved toroidal plasma current generally increases with increasing injector current. This is a good result as it suggests that spurious arcing may not be as severe as was originally hypothesized for this electrode configuration, but clearly requires more detailed studies in the future. In this experiment, peak toroidal currents up to 45 kA were measured in the plasma. The existence of toroidal current after the injector current is reduced to zero is an encouraging result that suggests the possibility of some current flowing on closed field lines in these initial transient CHI generated plasmas on QUEST, although at this time, the possibility of this current being induced by the decaying CHI plasma cannot be disputed. The demonstration of unambiguous closed flux generation is the next step for the CHI program on QUEST.

Acknowledgments

This work is supported by US DOE grants (DE-FG02-99ER54519 and DE-AC02-09CH11466), NIFS Collaboration Research Program (NIFS14KUTR103) and the Collaborative Research Program of Research Institute for Applied Mechanics, Kyushu University (international collaboration frame work No. 9 in 2016 and No. 8 in 2017). This work was partially supported by a Grant-in-Aid for JSPS Fellows (KAKENHI Grant Number 16H02441, 24656559), the NIFS Collaboration Research Program (NIFS05KUTRO14, NIFS13KUTR093, NIFS13KUTR085) and Japan/US Cooperation in Fusion Research and Development.

ORCID iDs

K Kuroda  <https://orcid.org/0000-0003-2451-4893>
 R Raman  <https://orcid.org/0000-0002-2027-3271>
 T R Jarboe  <https://orcid.org/0000-0001-7840-5524>
 A Fukuyama  <https://orcid.org/0000-0001-6204-9211>

References

- [1] Shiraiwa S *et al* 2004 *Phys. Rev. Lett.* **92** 035001
- [2] Menard J *et al* 2016 *Nucl. Fusion* **56** 106023
- [3] Uchida M, Yoshinaga T, Tanaka H and Maekawa T 2010 *Phys. Rev. Lett.* **104** 065001
- [4] Shevchenko V F, O'Brien M R, Taylor D, Saveliev A N and MAST team 2010 *Nucl. Fusion* **50** 022004
- [5] Hanada K *et al* 2011 *Plasma Sci. Technol.* **13** 307
- [6] Ishiguro M *et al* 2012 *Phys. Plasmas* **19** 062508
- [7] Poli F M, Andre R G, Bertelli N, Gerhardt S P, Mueller D and Taylor G 2015 *Nucl. Fusion* **55** 123011
- [8] Raman R *et al* 2013 *Nucl. Fusion* **53** 073017
- [9] Stork D *et al* 2010 *Proc. on 23th IAEA Fusion Energy Conf. (Daejeon, 2010)* ICC/P5-06
- [10] Raman R, Jarboe T R, Nelson B A, Hamp W T, Izzo V A, O'Neill R G, Redd A J, Sieck P E and Smith R J 2004 *Phys. Plasmas* **11** 2565
- [11] Jarboe T R 1989 *Fusion Sci. Technol.* **15** 7
- [12] Raman R, Jardin S C, Menard J, Jarboe T R, Bell M, Mueller D, Nelson B A and Ono M 2011 *Nucl. Fusion* **51** 113018
- [13] Ebrahimi F and Raman R 2016 *Nucl. Fusion* **56** 044002
- [14] Raman R *et al* 2011 *Phys. Plasmas* **18** 092504
- [15] Nelson B A *et al* 2011 *Nucl. Fusion* **51** 063008
- [16] Hanada K *et al* 2010 *Plasma. Fusion. Res.* **5** S1007
- [17] Hanada K *et al* 2017 *Nucl. Fusion* **57** 126061
- [18] Hanada K 2016 *Plasma Sci. Technol.* **18** 1069
- [19] Hanada K *et al* 2016 *Proc. on 26th IAEA Fusion Energy Conf. (Kyoto, 2016)* EX/P4-49
- [20] Idei H *et al* 2014 *Proc. on 25th IAEA Fusion Energy Conf. (Saint Petersburg, 2014)* EX/P1-38
- [21] Idei H *et al* 2017 *Nucl. Fusion* **57** 126045
- [22] Idei H *et al* 2012 *IEEEJ Trans. Fundam. Mater.* **132** 511
- [23] Kariya T 2015 *Trans. Fusion Sci. Technol.* **68** 147
- [24] Raman R, Brown T, El-Guebalay L A, Jarboe T R, Nelson B A and Menard J E 2015 *Fusion Sci. Technol.* **68** 674
- [25] Kuroda K *et al* 2017 *Plasma. Fusion. Res.* **12** 1202020
- [26] Jarboe T R, Bohnet M A, Mattick A T, Nelson B A and Orvis D J 1998 *Phys. Plasmas* **5** 1807
- [27] Redd A J, Jarboe T R, Nelson B A, O'Neill R G and Smith R J 2007 *Phys. Plasmas* **14** 112511
- [28] Raman R *et al* 2001 *Plasma Phys. Control. Fusion* **43** 305
- [29] Brown T, Menard J, El Gueblay L and Davis A 2015 *Fusion Sci. Technol.* **68** 277
- [30] Von Engel A 1983 *Electric Plasmas: Their Nature and Uses* (London: Taylor and Francis)
- [31] Hammond K C, Raman R and Volpe F A 2018 *Nucl. Fusion* **58** 016013
- [32] Raman R *et al* 2007 *Nucl. Fusion* **47** 792
- [33] Ebrahimi F and Raman R 2015 *Phys. Rev. Lett.* **114** 205003